



## SMART WIRELESS EV CHARGING USING NEURAL NETWORKS FOR REAL TIME IMPEDANCE CONTROL

**K. Vijayakanth\*, P. Aravinth\*\*, S. Gajendran\*\*, R. Makeshwaran\*\* & S. Mohan Dass\*\***

\* Assistant Professor, Department of Electrical and Electronics Engineering, Dhanalakshmi Srinivasan Engineering College (Autonomous), Perambalur, Tamil Nadu, India

\*\* UG Student, Department of Electrical and Electronics Engineering, Dhanalakshmi Srinivasan Engineering College (Autonomous), Perambalur, Tamil Nadu, India

**Cite This Article:** K. Vijayakanth, P. Aravinth, S. Gajendran, R. Makeshwaran & S. Mohan Dass, "Smart Wireless EV Charging Using Neural Networks for Real Time Impedance Control", International Journal of Engineering Research and Modern Education, Volume 11, Issue 1, January - June, Page Number 62-66, 2026.

**Copy Right:** © Crystal Pen Publication, 2026 (All Rights Reserved). This is an Open Access Article distributed under the Creative Commons Attribution License, which permits unrestricted use, distribution, and reproduction in any medium, provided the original work is properly cited.

**Type of Review:** Peer Reviewed as per |C|O|P|E| Guidance.

**Disclaimer:** The scholarly papers reviewed and published by Crystal Pen Publication, India, reflect the views and opinions of their respective authors and do not necessarily represent the views or opinions of Crystal Pen Publication. The publisher disclaims any responsibility for any harm, loss, or damage resulting from the use of the published content by any party.

**DOI:** <https://doi.org/10.5281/zenodo.19783193>

### Abstract:

Electric Vehicle wireless charging efficiency is highly sensitive to impedance mismatch caused by coil misalignment and varying operating conditions. An Artificial Neural Network based control strategy is proposed for optimal load impedance tracking in a Series-Series compensated Wireless Power Transfer system, replacing conventional mathematical methods that rely on the simplified assumption of negligible coil resistance. This assumption introduces estimation errors under practical operating conditions, particularly during coil misalignment and thermal variations. The proposed method replaces the mathematical tracking equations with a trained feed forward Artificial Neural Network having a four input, two hidden layers, two output architecture. The network takes four measured electrical parameters, namely transmitter voltage, transmitter current, receiver voltage, and receiver current, as inputs and simultaneously predicts the optimal PWM switching frequency and inverter duty cycle as dual outputs. Training data of 245 samples is generated by sweeping the coupling coefficient, load resistance, and input voltage across their operating ranges using the Series-Series circuit analytical model in MATLAB. The network is trained using the Levenberg-Marquardt algorithm with early stopping. The trained model is deployed on an ESP32-S3 microcontroller using Tensor Flow Lite Micro, enabling real time inference at low cost. Receiver side measurements are transmitted to the transmitter controller via the ESP-NOW wireless protocol from an ESP32-C3 sensor node. Simulation results demonstrate that the proposed ANN control achieves an average efficiency improvement of 0.12% over the conventional mathematical method across all tested coupling coefficients. The system operates at 50 W and 85 kHz in full compliance with the SAE J2954 wireless charging standard.

**Key Words:** Wireless Power Transfer, Artificial Neural Network, Impedance Matching, Electric Vehicle Charging, Series-Series Topology, ESP32-S3, Tensor Flow Lite Micro, Levenberg-Marquardt, Optimal Load Control.

### INTRODUCTION:

The global transition toward sustainable transportation has accelerated the adoption of Electric Vehicles (EVs) as a primary solution to reduce carbon emissions and dependence on fossil fuels. As EV adoption grows rapidly across both developed and developing regions, the demand for efficient, safe, and convenient charging infrastructure has become a critical engineering challenge. Conventional wired charging systems, while effective, suffer from mechanical wear due to repeated connector use, safety concerns in outdoor and wet environments, and practical inconvenience for users. These limitations have motivated significant research interest in Wireless Power Transfer (WPT) technology, which enables contactless energy transfer between a ground mounted transmitter coil and a vehicle mounted receiver coil without any physical connection.

Despite the advantages of WPT technology, maintaining maximum power transfer efficiency under varying operating conditions remains a fundamental control challenge. The coupling coefficient between the transmitter and receiver coils changes with vehicle positioning and lateral misalignment. The battery equivalent resistance changes continuously throughout the charging session as the battery transitions from Constant Current to Constant Voltage charging mode. These variations continuously shift the system away from its optimal operating point, causing efficiency degradation if the control system does not compensate in real time.

Zavrel, Drabek, Kindl, and Frivaldsky [1] presented a 65-kW wireless charging station using mathematical optimal impedance tracking, where the optimal load resistance ( $R_L$ ) is defined as:

$$R_L(\eta \rightarrow \max) = M \cdot \omega_0 \quad (1)$$

Where  $M$  is mutual inductance and  $\omega_0 = 2\pi f_0$  is the angular resonant frequency.  $M$  is estimated from DC measurements using:

$$M_{(t+1)} = \sqrt{[R_{L(t)} \cdot Z_{te(t)}] / \omega_{(t)}^2} \quad (2)$$

The equivalent TX (transmitter side) impedance  $Z_{te}$  and load resistance  $R_L$  are from:

$$Z_{te} = (\pi/4) \cdot (u_{DC1}/i_{DC1}) \quad (3)$$

$$R_L = (8/\pi^2) \cdot (u_{DC2}/i_{DC2}) \quad (4)$$

The limitation is that equation 1 is derived under the assumption  $R_x \rightarrow 0$  (negligible coil resistance). In practice,  $R_x$  is non-negligible, especially at low coupling coefficients ( $k = 0.10-0.20$ ) representing coil misalignment. This introduces systematic underestimation of  $R_{L(opt)}$ , reducing efficiency. To overcome this limitation, the present work proposes a trained Artificial Neural Network as a direct replacement for equations 1-4, eliminating the  $R_x \rightarrow 0$  assumption and enabling accurate impedance tracking under all operating conditions.

**Related Works:**

Various research works related to wireless power transfer systems, impedance matching techniques, and artificial neural network based control are reviewed in this section.

**A. Wireless Power Transfer System Design and Topology:**

Li and Mi [8] survey wireless power transfer technologies for electric vehicle applications and concluded that the Series-Series topology offers the best combination of load-independent resonant frequency and simplified control architecture for static electric vehicle charging, directly justifying the topology selection in the present work. Kindl, Frivaldsky, Zavrel, and Pavelek [5] present a generalized design methodology for Series-Series wireless chargers, establishing the component relationships used in the present work, specifically 100  $\mu\text{H}$  coil inductance, 35.1 nF resonant capacitors, and 85 kHz operating frequency. Zhang, Wong, Tse, and Chen [4] prove analytically that maximum efficiency in Series-Series systems occurs when the load resistance equals  $\sqrt{(R_x^2 + M^2\omega^2)}$ , which is the true optimal expression that the proposed ANN is trained to predict and directly exposes the limitation of the simplified expression in [1] that ignores the coil resistance term. The SAE J2954 standard [10] defines the 79 to 90 kHz operating band and interoperability requirements within which the proposed system fully operates. These design principles and standards form the theoretical and regulatory foundation of the proposed 50 W Series-Series wireless power transfer system.

**B. Impedance Matching and Optimal Load Control:**

Zavrel et al. [1] demonstrate a 65-kW wireless charging station where the Buck-Boost DC-DC converter duty cycle is adjusted every control cycle using mutual inductance estimated from DC measurements, achieving over 95.5% efficiency. However, the method assumes negligible coil resistance, introducing estimation errors under misalignment and thermal variations that the present work directly addresses. Bui et al. [6] demonstrate that DC-DC converter duty cycle control achieves near-maximum power transfer efficiency through resistance emulation, validating the impedance matching principle adopted in the present work. Berger et al. [3] establish that simultaneously controlling two variables eliminates the trade-off between efficiency and power maximization inherent in single variable control, providing strong justification for the dual output ANN design proposed in this paper. Mai et al. [12] propose an active rectifier based maximum efficiency tracking method, validating the objective of real-time optimal impedance control. Kavimandan et al. [17] quantify significant efficiency degradation at low coupling coefficients representing coil misalignment, establishing the sensitivity problem that the present ANN controller specifically addresses across the full coupling range from 0.10 to 0.40. These works collectively validate the Buck-Boost duty cycle as the appropriate impedance matching variable and confirm that dual variable control outperforms single variable methods.

**C. Frequency Optimization and Efficiency Tracking:**

Kindl, Zavrel, Drabek, and Kavalir [11] present a phase shift control method for wireless charging efficiency optimization, establishing the baseline control approach that the impedance tracking method of [1] subsequently improves upon and motivating the further improvement through dual output ANN control in the present work. Jiao et al. [13] demonstrate that the actual resonant frequency of a practical wireless power transfer system deviates from its nominal design value due to coupling variation and component tolerances, and that tracking this actual frequency provides measurable efficiency gains over fixed frequency operation particularly under misalignment conditions. Wang et al. [18] confirm that both active impedance matching and frequency tuning are necessary for achieving maximum efficiency at the 50 W scale, directly corresponding to the operating scale of the present work. Zhao et al. [20] confirms that frequency based efficiency optimization is computationally feasible in real-time embedded systems. These findings establish that fixing the switching frequency at 85 kHz as the mathematical method of [1] does leaves measurable efficiency gains unrealized, directly justifying the inclusion of switching frequency as the second output of the proposed ANN controller.

**D. Artificial Neural Networks in Wireless Power Transfer:**

Amadei, Quercio, and Riganti Fulginei [2] review artificial intelligence techniques applied to wireless power transfer systems and demonstrate that feed forward neural networks trained on simulation data can learn nonlinear control mappings and deploy on embedded microcontrollers for real-time operation. The review identifies that most existing ANN applications optimise only a single output variable, directly motivating the dual output architecture proposed in the present work. Amadei et al. [19] further demonstrate neural network based misalignment detection using only standard voltage and current measurements, confirming that the four electrical inputs adopted in the present work are sufficient for accurate neural network based control across variable coupling conditions. Hagan and Menhaj [9] establish that the Levenberg-Marquardt algorithm achieves near-quadratic convergence for small regression problems, making it the most appropriate training choice for the 245-sample dataset and 234-parameter network used in this work.

**Proposed System:**

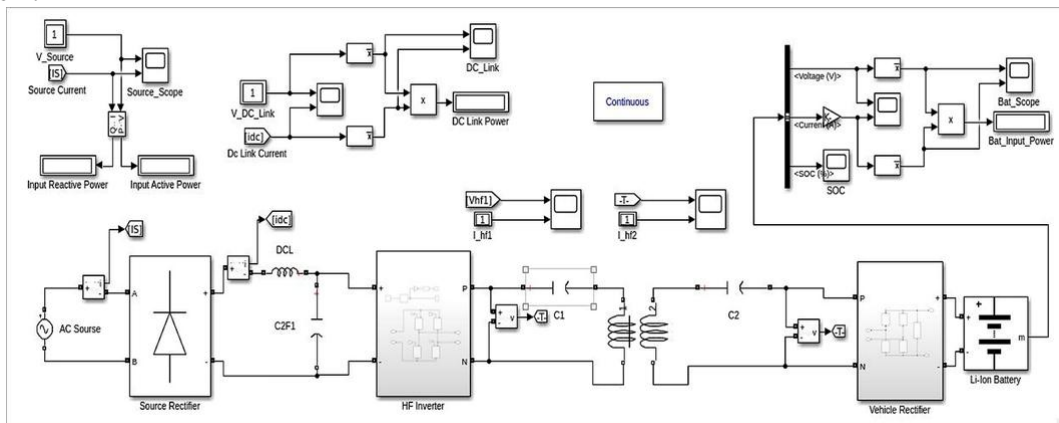


Figure 1: Simulation diagram

The system operates at 50 W with 24-48 V variable DC input, 85 kHz resonant frequency, and S-S topology. Coil inductance  $L_1 = L_2 = 100 \mu\text{H}$ , resonant capacitors  $C_1 = C_2 = 35.1 \text{ nF}$ , coupling coefficient  $k \in [0.10, 0.40]$ , air gap 15-25 cm.

TX (Transmitter Side): H-Bridge inverter (IRLZ44N  $\times 4$ , IR2104), INA219 sensors for transmitter side voltage  $V_{tx}$  and transmitter side current  $I_{tx}$ , ESP32-S3 running ANN via Tensor Flow Lite Micro, OLED display.

RX (Receiver Side): Full-bridge rectifier, Buck-Boost DC-DC converter for impedance matching, INA219 sensors for receiver side voltage  $V_r$  and receiver side current  $I_r$ , ESP32-C3 transmitting measurements via ESP-NOW (1-5 ms latency).

The proposed approach eliminates the  $R_x \rightarrow 0$  assumption by substituting equations 1-4 with a data-driven Artificial Neural Network trained on simulation data generated using the complete circuit model. The true optimal  $R_L$  (including  $R_x$ ) is:

$$R_L(\eta \rightarrow \max) = \sqrt{(R_x^2 + M^2 \omega_0^2)}(5)$$

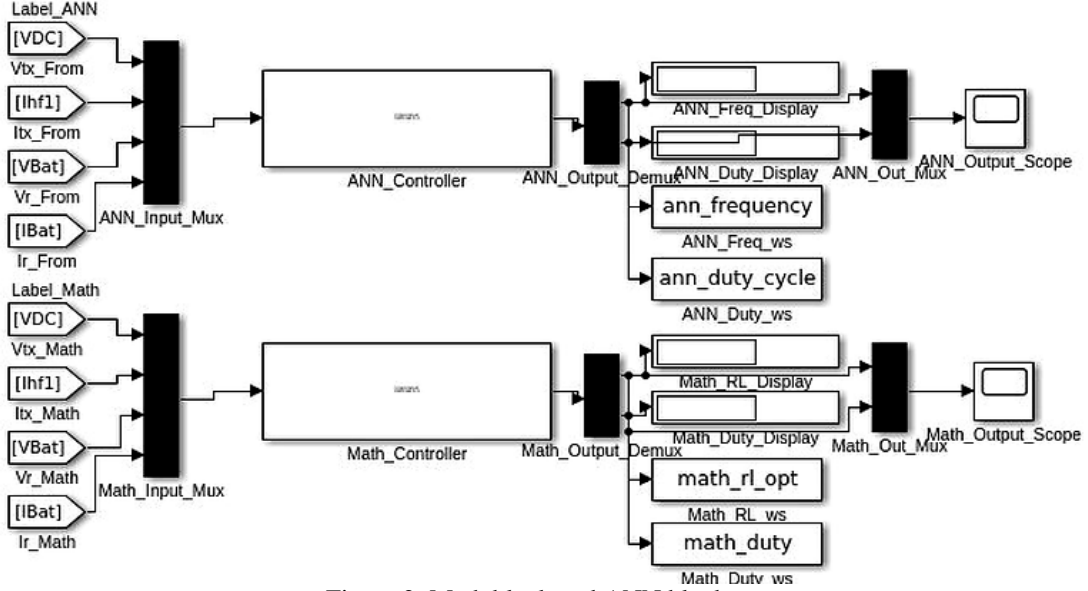


Figure 2: Math block and ANN block

The ANN learns this nonlinear mapping directly from data, eliminating the  $R_x \rightarrow 0$  assumption. It simultaneously predicts optimal PWM frequency  $f_{opt}$  and converter duty cycle  $z$ , providing dual-variable control not available in the mathematical method.

#### ANN Architecture & Training:

The ANN has the structure:  $4 \rightarrow 16 \rightarrow 8 \rightarrow 2$ , with 234 trainable parameters. Hidden layers use TanSig ( $\phi = \tanh$ ) activation; output layer uses LogSig (sigmoid, bounds outputs to  $[0, 1]$ ).

Table 1: ANN architecture

| Layer         | Details                                 |
|---------------|---|
| Input (4)     | $V_{tx}, I_{tx}, V_r, I_r$              |
| Hidden 1 (16) | TanSig activation                       |
| Hidden 2 (8)  | TanSig activation                       |
| Output (2)    | $f_{opt}, z$ LogSig                     |
| Algorithm     | Levenberg-Marquardt                     |
| Samples       | 245 ( $7k \times 7R_L \times 5V_{dc}$ ) |
| Split         | 70/15/15 train/val/test                 |
| MSE target    | $1 \times 10^{-5}$                      |

Training data generated by sweeping  $k \in \{0.10, 0.15, 0.20, 0.25, 0.30, 0.35, 0.40\}$ ,  $R_L \in \{5, 8, 11, 14, 17, 20, 23\} \Omega$ ,  $V_{dc} \in \{24, 30, 36, 42, 48\} \text{ V}$ . For each sample, inputs ( $V_{tx}, I_{tx}, V_r, I_r$ ) and labels ( $f_{opt}, z$ ) are computed from the full S-S circuit equations including  $R_x = \omega_0 L / Q$  where  $Q = 50$ .

The network is trained in MATLAB using the fitnet function from the Neural Network Toolbox with the Levenberg-Marquardt algorithm selected through the trainlm option. The Levenberg-Marquardt algorithm is a second order optimization method that combines the stability of gradient descent with the fast convergence of the Gauss-Newton method by maintaining an approximation of the Hessian matrix. This makes it significantly faster than first order methods such as Adam or stochastic gradient descent for small regression problems, typically converging in fewer than 100 epochs for the 245-sample dataset used here. The 245 samples are divided into 70 percent for training (171 samples), 15 percent for validation (37 samples), and 15 percent for testing (37 samples). Early stopping with a patience of 20 epochs monitors the validation set mean squared error and restores the best weights when validation performance stops improving, preventing over fitting despite the small dataset size.

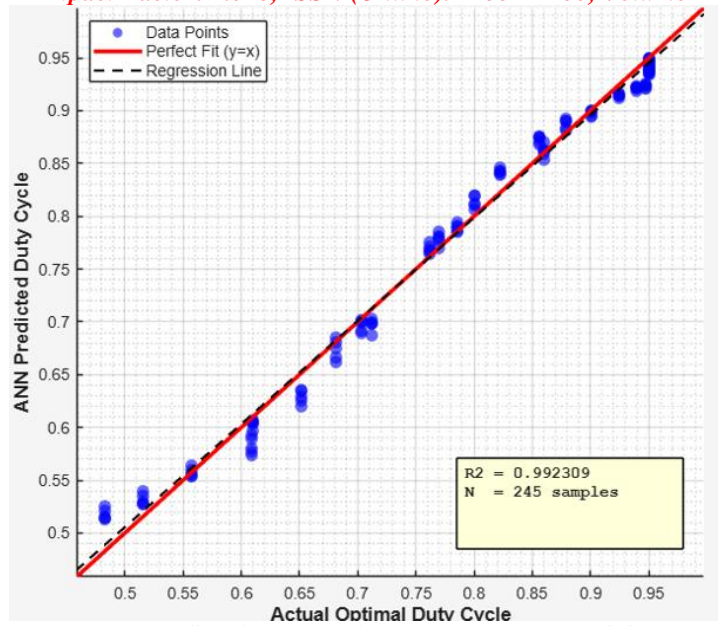


Figure 3: ANN Predicted Duty Cycle vs Target Across Training Samples

**Simulation Results:**

The WPT system is modelled analytically in MATLAB using the S-S circuit equations. Coil resistance  $R_x = \omega_0 L/Q \approx 1.07 \Omega$  at  $f_0 = 85 \text{ kHz}$ ,  $L = 100 \mu\text{H}$ ,  $Q = 50$ . Three methods are compared.

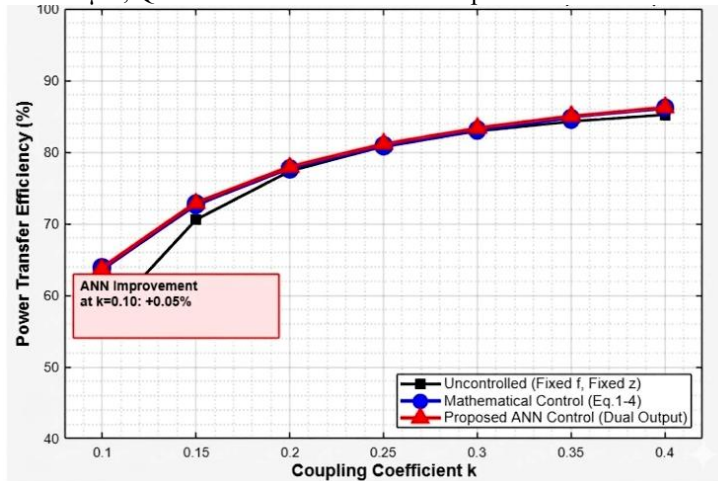


Figure 4: Uncontrolled vs Mathematical control vs ANN control

The ANN converged with (Mean Squared Error)  $MSE < 10^{-5}$  on all subsets.  $R^2 > 0.99$  for both outputs confirms accurate prediction across the full operating range.

Unlike the mathematical method which controls only duty cycle  $z$  at a fixed 85 kHz, the ANN simultaneously predicts both optimal frequency  $f_{opt}$  and duty cycle  $z$ . This dual-output control compensates for resonant frequency shifts caused by coupling variation, providing additional efficiency gains that the fixed-frequency mathematical method cannot achieve.

The ANN achieved training MSE of  $5.21 \times 10^{-4}$  with validation and test MSE closely aligned, confirming no over fitting despite only 245 training samples.  $R^2$  values of 0.9923 for duty cycle and 0.9948 for frequency prediction confirm that the model generalizes accurately across the full operating range.

Table 2: Simulation Results Comparison

| Metric                                   | Math      | ANN                   |
|--|-----------|-----------------------|
| $\eta$ at $k=0.40$ , $V_{ac}=36\text{V}$ | 85.96%    | 86.15%                |
| $\eta$ at $k=0.25$ , $V_{ac}=36\text{V}$ | 80.97%    | 81.09%                |
| $\eta$ at $k=0.10$ , $V_{ac}=36\text{V}$ | 63.84%    | 63.89%                |
| Avg. improvement                         | baseline  | 0.12%                 |
| $R^2$ duty cycle $z$                     |           | 0.992309              |
| $R^2$ frequency $f$                      |           | 0.994832              |
| ANN Training MSE                         |           | $5.21 \times 10^{-4}$ |
| Control variables                        | 1 ( $z$ ) | 2 ( $f, z$ )          |
| $R_x \rightarrow 0$ assumption           | Yes       | Not needed            |

Figure 6 shows efficiency  $\eta$  vs. coupling coefficient  $k$  at  $V_{dc} = 36 \text{ V}$ . The ANN achieves the highest efficiency at all  $k$  values. The improvement is largest at  $k=0.10$  (misalignment), where the  $R_x \rightarrow 0$  assumption causes the greatest error in equation 1. Specifically, the simplified expression underestimates  $R_{L(opt)}$ , causing the DC-DC converter to present a sub-optimal

impedance to the resonant circuit. The ANN avoids this by learning the true  $R_{L(opt)}$  from training data generated with full coil resistance included.

The achieved training MSE of  $5.21 \times 10^{-4}$  exceeded the initial target of  $1 \times 10^{-5}$ , however the  $R^2$  values of 0.9923 and 0.9948 confirm that this MSE level is sufficient for accurate impedance tracking control within the operating range of this system.

At  $k = 0.25-0.40$ , both methods converge toward similar efficiency because  $R_x$  becomes proportionally smaller relative to  $M\omega_0$ , validating that the  $R_x \rightarrow 0$  assumption holds well only at high coupling. The dual-output ANN provides additional gain by also correcting for the resonant frequency shift caused by coupling variation, which the mathematical method ignores by fixing  $f = 85$  kHz.

#### **Conclusion:**

This paper demonstrated that a  $4 \rightarrow 16 \rightarrow 8 \rightarrow 2$  ANN trained using the Levenberg-Marquardt algorithm can replace the mathematical impedance tracking equations (Eq. 1-4) in an S-S WPT system. The ANN achieved  $R^2 > 0.99$  for both output variables. Simulation confirmed higher  $\eta$  than the mathematical method across  $k \in [0.10, 0.40]$  and  $V_{dc} \in [24, 48]$  V, with the greatest improvement at low  $k$  (misalignment). Deployment on ESP32-S3 using Tensor Flow Lite Micro confirms feasibility at minimal cost. Future work includes hardware prototype construction and scaling to higher power levels (500 W, 1 kW).

#### **References:**

1. M. Zavrel, P. Drabek, V. Kindl, and M. Frivaldsky, "Design of a 65-kW Wireless Charging Station Characterized by Optimal Load Impedance Tracking Control," *IEEE Open J. Veh. Technol.*, vol. 6, pp. 2462-2478, 2025.
2. F. Amadei, M. Quercio, and F. RigantiFulginei, "Recent Results on AI Techniques Applied to WPT Systems," *IEEE Access*, vol. 13, pp. 58443-58464, 2025.
3. A. Berger et al., "A Wireless Charging System Applying Phase-Shift and Amplitude Control," *IEEE Trans. Power Electron.*, vol. 30, no. 11, pp. 6338-6348, 2015.
4. W. Zhang, S. C. Wong, C. K. Tse, and Q. Chen, "Design for Efficiency Optimization of S-S IPT Systems," *IEEE Trans. Power Electron.*, vol. 29, no. 1, pp. 191-200, 2014.
5. V. Kindl, M. Frivaldsky, M. Zavrel, and M. Pavelek, "Generalized Design Approach on Industrial Wireless Chargers," *Energies*, vol. 13, Art. No. 2697, 2020.
6. D. Bui, T. M. Mostafa, A. P. Hu, and R. Hattori, "DC-DC Converter Based Impedance Matching for Maximum Power Transfer," *IEEE WoW*, 2018.
7. V. Ramakrishnan et al., "A Comprehensive Review on Efficiency Enhancement of Wireless Charging for EVs," *IEEE Access*, vol. 12, pp. 46967-46994, 2024.
8. S. Li and C. C. Mi, "Wireless Power Transfer for Electric Vehicle Applications," *IEEE J. Emerg. Sel. Topics Power Electron.* vol. 3, no. 1, pp. 4-17, 2015.
9. M. T. Hagan and M. B. Menhaj, "Training Feed forward Networks with the Marquardt Algorithm," *IEEE Trans. Neural Netw.*, vol. 5, no. 6, pp. 989-993, 1994.
10. SAE International, "Wireless Power Transfer for Light-Duty Plug-In/Electric Vehicles and Alignment Methodology," *SAE Standard J2954*, 2020.
11. V. Kindl, M. Zavrel, P. Drabek, and T. Kavalir, "High Efficiency and Power Tracking Method for Wireless Charging System Based on Phase-Shift Control," *Energies*, vol. 11, Art. No. 2065, 2018.
12. R. Mai, Y. Liu, Y. Li, P. Yue, G. Cao, and Z. He, "An Active Rectifier-Based Maximum Efficiency Tracking Method Using an Additional Measurement Coil for Wireless Power Transfer," *IEEE Trans. Power Electron.*, vol. 33, no. 1, pp. 716-728, Jan. 2018.
13. S. Jiao, S. Li, L. Wang, and J. Wu, "An Optimal Frequency Control Strategy for Wireless Power Transfer System to Achieve Maximum Energy Efficiency," in *Proc. IEEE 7<sup>th</sup> Int. Elect. Energy Conf. (CIEEC)*, Harbin, China, 2024, pp. 1424-1430.
14. W. Wang, J. Deng, D. Chen, Z. Wang, and S. Wang, "A Novel Design Method of LCC-S Compensated Inductive Power Transfer System Combining Constant Current and Constant Voltage Mode via Frequency Switching," *IEEE Access*, vol. 9, pp. 117244-117256, 2021.
15. M. Bertoluzzo, A. Kumar, and A. Sagar, "Control Strategy for a Bidirectional Wireless Power Transfer System with Vehicle to Home Functionality," *IEEE Access*, vol. 11, pp. 60421-60448, 2023.
16. C. S. Wang, O. H. Stielau, and G. A. Covic, "Design Considerations for a Contactless Electric Vehicle Battery Charger," *IEEE Trans. Ind. Electron.*, vol. 52, no. 5, pp. 1308-1314, 2005.
17. U. D. Kavimandan, V. P. Galigekere, O. Onar, M. Mohammad, B. Ozpineci, and S. M. Mahajan, "The Sensitivity Analysis of Coil Misalignment for a 200-kW Dynamic Wireless Power Transfer System with an LCC-S Compensation," in *Proc. IEEE Transp. Electrific. Conf. Expo (ITEC)*, 2021, pp. 1-8.
18. Z. Wang, W. Luo, M. Ma, and Q. Liu, "Research on Efficiency Optimization of Medium and Small Power Wireless Energy Transfer," in *Proc. Chinese Control Decis. Conf. (CCDC)*, Hefei, China, 2020, pp. 3348-3353.
19. F. Amadei, M. Quercio, and F. Riganti Fulginei, "Neural Network Based Coil Misalignment Detection and Compensation in Wireless Power Transfer Systems for Electric Vehicles," *IEEE Trans. Magn.*, vol. 59, no. 5, pp. 1-5, May 2023.
20. R. Zhao, D. T. Gladwin, and D. A. Stone, "Phase Shift Control Based Maximum Efficiency Point Tracking in Resonant Wireless Power System and Its Realization," in *Proc. 42<sup>nd</sup> Annu. Conf. IEEE Ind. Electron. Soc. (IECON)*, Florence, Italy, 2016, pp. 4541-4546.